scientific reports

Check for updates

OPEN

IGF-I concentration determines cell fate by converting signaling dynamics as a bifurcation parameter in L6 myoblasts

Ryosuke Okino[1,6,10], Kazuaki Mukai[1,10], Shunpei Oguri[1], Masato Masuda[1,2], Satoshi Watanabe[3], Yosuke Yoneyama[1,4], Sumine Nagaosa[1], Takafumi Miyamoto[7,8,9], Atsushi Mochizuki[5], Shin-Ichiro Takahashi[1] & Fumihiko Hakuno[1,10]✉

Insulin-like growth factor (IGF)-I mediates long-term activities that determine cell fate, including cell proliferation and differentiation. This study aimed to characterize the mechanisms by which IGF-I determines cell fate from the aspect of IGF-I signaling dynamics. In L6 myoblasts, myogenic differentiation proceeded under low IGF-I levels, whereas proliferation was enhanced under high levels. Mathematical and experimental analyses revealed that IGF-I signaling oscillated at low IGF-I levels but remained constant at high levels, suggesting that differences in IGF-I signaling dynamics determine cell fate. We previously reported that differential insulin receptor substrate (IRS)-1 levels generate a driving force for cell competition. Computational simulations and immunofluorescence analyses revealed that asynchronous IRS-1 protein oscillations were synchronized during myogenic processes through cell competition. Disturbances of cell competition impaired signaling synchronization and cell fusion, indicating that synchronization of IGF-I signaling oscillation is critical for myoblast cell fusion to form multinucleate myotubes.

Keywords Insulin-like growth factor-I, Signaling dynamics, Signaling oscillation, Cell competition, L6 myoblast, Myogenesis, Bifurcation analysis

Insulin-like growth factor-I (IGF-I) is an anabolic hormone with a structure similar to proinsulin[1]. Insulin mediates acute metabolic functions, including glucose uptake in skeletal muscles and adipose tissues, whereas IGF-I mediates long-term actions that determine cell fate, including cell growth, differentiation, and cell survival[2]. However, it is unclear how IGF-I promotes cell proliferation and differentiation, which appear to have opposite bioactivities.

Skeletal muscle development is mediated by stem cells called satellite cells. Satellite cells proliferate and activate into myoblasts in response to physical stimuli or growth signaling[3]. IGF-I is essential for promoting satellite cell proliferation and activation into myoblasts[4–6]. Owing to this activity, muscle-specific IGF-I transgenic mice showed myofiber hypertrophy[7]. Contrarily, IGF-I receptor null mutant mice showed decreased muscle mass[8]. In the rat L6 myoblast cell line, IGF-I has also been shown to play critical roles in both myoblast differentiation and proliferation[9–12]. IGF-I stimulation induces cell growth[13], and in the absence of IGF-I, myogenic differentiation into myotubes does not occur. Moreover, adding an inhibitor of the p85 phosphatidylinositol 3-kinase (PI3K), one of the main IGF-I signaling pathways blocks both IGF-I-induced proliferation and differentiation[14]. Thus, the IGF-I hormone and its signaling activity are essential for both muscle proliferation and differentiation. Florini et al. showed a biphasic relationship between the concentration of IGF-I and the differentiation of L6 myoblasts.

[1]Department of Animal Resource Sciences, Graduate School of Agricultural and Life Sciences, The University of Tokyo, Tokyo, Japan. [2]Faculty of Information Sciences and Arts, Toyo University, Saitama, Japan. [3]Advanced Institute for Materials Research, Tohoku University, Sendai, Japan. [4]Institute of Research, Tokyo Medical and Dental University, Tokyo, Japan. [5]Laboratory of Mathematical Biology, Institute for Life and Medical Sciences, Kyoto University, Kyoto, Japan. [6]Muscle Biology Laboratory, Research Team for Aging Science, Tokyo Metropolitan Institute for Geriatric and Gerontology (TMIG), Tokyo, Japan. [7] Department of Endocrinology and Metabolism, Institute of Medicine, University of Tsukuba, Ibaraki, Japan. [8] Transborder Medical Research Center, University of Tsukuba, Ibaraki, Japan. [9] Cybermedicine Research Center, University of Tsukuba, Ibaraki, Japan. [10]These authors contributed equally: Ryosuke Okino, Kazuaki Mukai and Fumihiko Hakuno. ✉email: hakuno@g.ecc.u-tokyo.ac.jp

Muscle differentiation was not induced without IGF-I but inhibited at high concentrations[15]. However, the differences in IGF-I signaling activity during muscle differentiation and proliferation are unknown.

Generally, after binding to specific receptors on the plasma membrane, IGF-I activates its intrinsic tyrosine kinase activity[16,17]. The activated receptors phosphorylate several intracellular substrates, including insulin receptor substrates (IRSs)[18]. Tyrosine phosphorylation of IRSs leads to their binding to several intermediate signaling molecules containing Src homology 2 domains, including PI3K regulatory subunit and Grb2. Subsequently, signaling pathways, such as the PI3K and Ras-MAPK cascades, are activated[19–21]. Accumulated data indicate that activation of these pathways is required for IGF-I bioactivity. In particular, activated PI3K generates phosphatidylinositol-3,4,5-triphosphate, leading to the activation of Ser/Thr kinase Akt. Activated Akt then activates the mechanistic target of rapamycin complex 1 (mTORC1) via phosphorylation-mediated suppression of the tuberous sclerosis complex protein complex, which inhibits the small GTPase, Rheb, an essential activator of mTORC1. The mTORC1 regulates many activities of IGF-I by phosphorylating distinct substrates, including S6 kinase 1, to regulate protein translation, autophagy, and cell growth.

Furthermore, the downregulation mechanism of the IGF-I signaling pathway has been extensively studied. Some studies have reported that IRS-1, an IRS family protein, is degraded by IGF-I/insulin signaling activation. IRS-1 was degraded via the ubiquitin-mediated 26S proteasome, and this degradation was blocked by the inhibition of phosphatidylinositol 3′-kinase activity[22]. The protein levels of IRS-1 are also decreased by the downstream kinase, mTORC1. The serine phosphorylation of IRS-1 via active mTORC1 recruits the $SCF^{\beta\text{-}TRCP}$ E3 ligase complex, catalyzing IRS-1 degradation[23]. As IRS-1 is an important mediator of IGF-I signaling, it is widely accepted that a decrease in IRS-1 protein levels is one of the mechanism involved in the downregulation of IGF-I signaling. However, recently, we reported a novel function for IRS-1 related to IGF-I signaling desensitization in L6 myoblasts: IRS-1 associates with the medium chain of the clathrin-coated adapter protein, AP2 and competitively inhibits its function. This process suppresses the internalization of active IGF-I receptors on the plasma membrane[24]. This novel downregulation mechanism does not rely on IRS-1's role as a signaling mediator but instead reveals a novel function that modulates IGF-I receptor internalization.

Recently, we reported that differences in IRS-1 protein levels induce cell competition during myogenesis in L6 myoblasts. Briefly, cells with high IRS-1 levels are eliminated from the cell layer via cell competition[25]. Cell competition is a cell fitness-sensing mechanism whereby less fit cells are eliminated as 'losers' when surrounded by more fit cells, the 'winners'[26,27]. However, the biological significance of cell competition driven by differential expression levels of IRS-1 during myogenic differentiation remains unclear.

In this study, we investigated the detailed mechanisms by which IGF-I determines different cell fates from the aspect of IGF-I signaling dynamics. IGF-I concentration was revealed to be a bifurcation parameter for determining whether the IGF-I signaling oscillates or remains constant. In addition, proliferation was induced when the IGF-I signaling was constant, and differentiation was induced when it oscillated. These results strongly suggest that IGF-I concentration determines cell fate by altering IGF-I signaling dynamics. In addition, IRS-1 oscillations were synchronized via cell competition in a cell-autonomous manner, and this IGF-I signaling synchronization is critical for cell fusion to form multinucleate myotubes.

Results

High concentration of IGF-I inhibited myogenic differentiation but enhanced proliferation

IGF-I is essential for the proliferation and differentiation of L6 myoblasts. Studies have shown that muscle differentiation is inhibited at high IGF-I concentrations[15]. Thus, we examined proliferation and differentiation abilities in L6 myoblasts at high and low IGF-I concentrations. Confluent L6 myoblasts were differentiated into myotubes by exchanging Dulbecco's modified Eagle medium (DMEM) supplemented with 10% fetal bovine serum (FBS) for DMEM with 2% FBS (differentiation medium) containing 0 or 100 ng/mL IGF-I. Two days after the induction of differentiation, the expression of the myogenic marker protein, MyHC (Myosin Heavy Chain), was induced in the differentiation medium that did not contain IGF-I. However, when 100 ng/mL IGF-I was added to the differentiation medium, MyHC expression was impaired (Fig. 1A), indicating that a high concentration of IGF-I inhibited myogenic differentiation. Expression levels of the myogenic master transcription factor, myogenin, were also impaired after the addition of 100 ng/mL IGF-I on the second day. Furthermore, the fusion index, which indicates the differentiation level of myoblasts into multinucleate myotube cells, was impaired after adding 100 ng/mL IGF-I (Fig. 1B,C). Next, their proliferative abilities under the same conditions were examined. [^{3}H]-labeled thymidine was added to the medium for 4 h, whereafter the [^{3}H] incorporated into DNA was measured as an indicator of proliferation ability. When L6 myoblasts were cultured in DMEM with 2% FBS containing 0, 1, or 10 ng/mL IGF-I, cell proliferation ability was weak. However, cell proliferation was enhanced when cultured in DMEM with 2% FBS containing 100 ng/mL IGF-I (Fig. 1D). Thus, the myoblast cell fate switched in the presence of different concentrations of IGF-I. To investigate the molecular mechanism by which IGF-I concentration switches the cell fate of L6 myoblasts, we analyzed whether the activation dynamics of IGF-I signaling were affected by differences in the IGF-I concentration.

Mathematical model of IGF-I signaling

We constructed a mathematical model of IGF-I signaling. Recently, we reported a novel regulatory mechanism of the IGF-I signaling pathway in L6 myoblasts. Briefly, (1) IRS-1 interferes with IGF-I receptor internalization through competitively inhibiting AP2 function[24]. (2) IRS-1 protein levels are downregulated by active mTORC1 kinase[23]. As IGF-I signaling is known to be downregulated by IGF-I receptor internalization, high IRS-1 levels lead to their sustained activation. Thus, in this model, IRS-1 is not a mediator, but rather a regulator that modulates the duration of IGF-I signaling pathway activity (Fig. 2A).

We modeled the IGF-I signaling pathways using the form of ordinary differential equations (Fig. 2B):

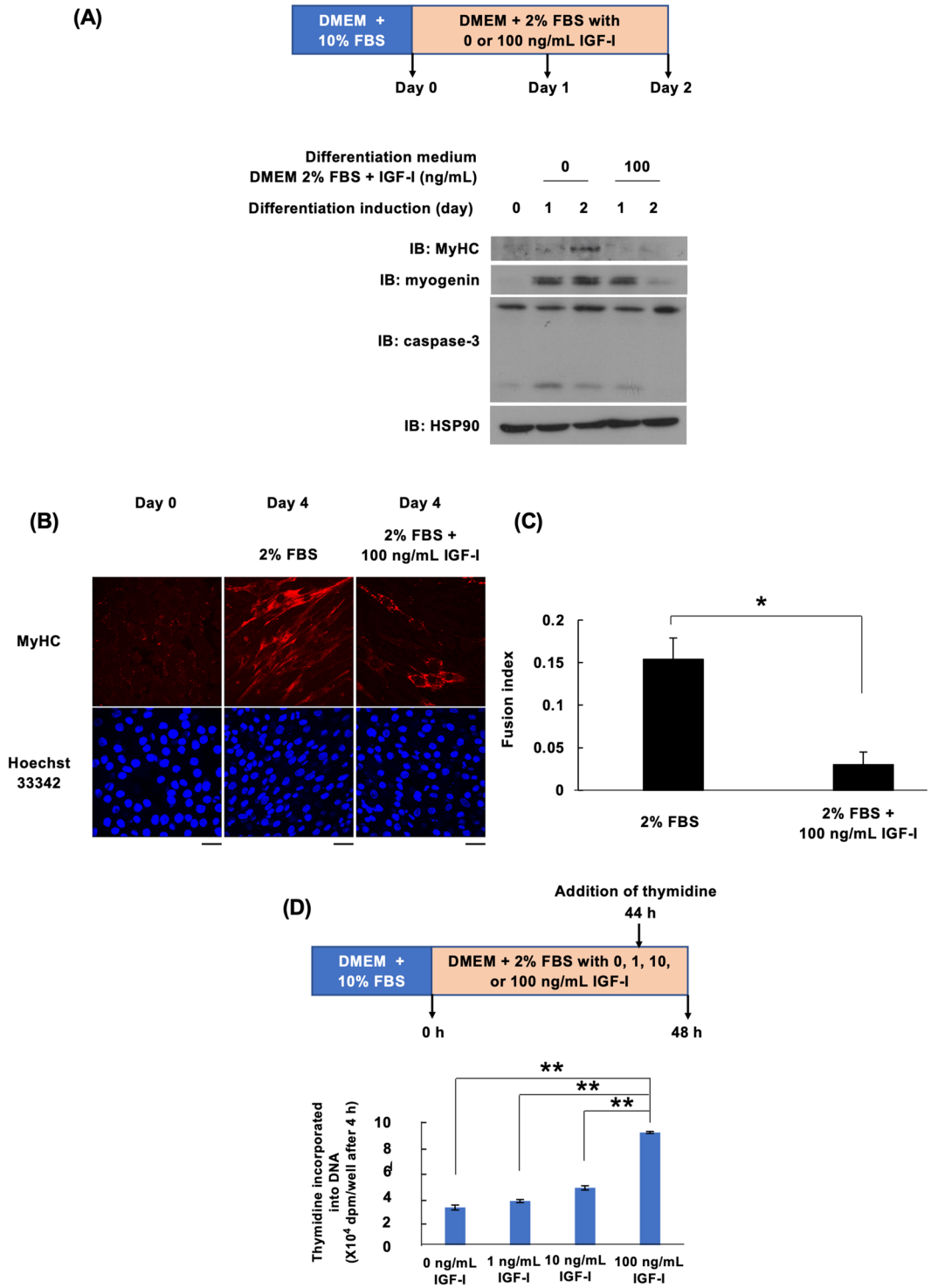

Fig. 1. Effects of IGF-I concentration on IGF-I signaling pathway dynamics and bioactivity expression. (**A**) L6 myoblasts were incubated in a differentiation medium (DMEM with 2% fetal bovine serum (FBS)) supplemented with either 0 or 100 ng/mL insulin-like growth factor-I (IGF-I). Cell lysates were collected at 0, 1, or 2 days post-differentiation induction for immunoblotting analysis using the specified antibody. (**B**) L6 myoblasts were cultured in a differentiation medium. Cells were fixed with 4% paraformaldehyde at 0 and 4 days post-differentiation induction and subjected to immunostaining analysis using the MyHC antibody. Scale bar = 50 µm. (**C**) The fusion index was determined (n = 3). Data are presented as mean ± SEM. *P < 0.05, determined by Student's t-test. (**D**) L6 myoblasts were cultured in a differentiation medium (DMEM with 2% FBS) supplemented with 0, 1, 10, or 100 ng/mL IGF-I. Forty-four hours later, [methyl-^{3}H] thymidine was added, and after a 4-h incubation, the amount of [^{3}H] incorporated into DNA was measured as an indicator of proliferation ability (n = 6). Data are presented as mean ± SEM. **P < 0.01, analyzed using one-way ANOVA followed by Tukey's post hoc test.

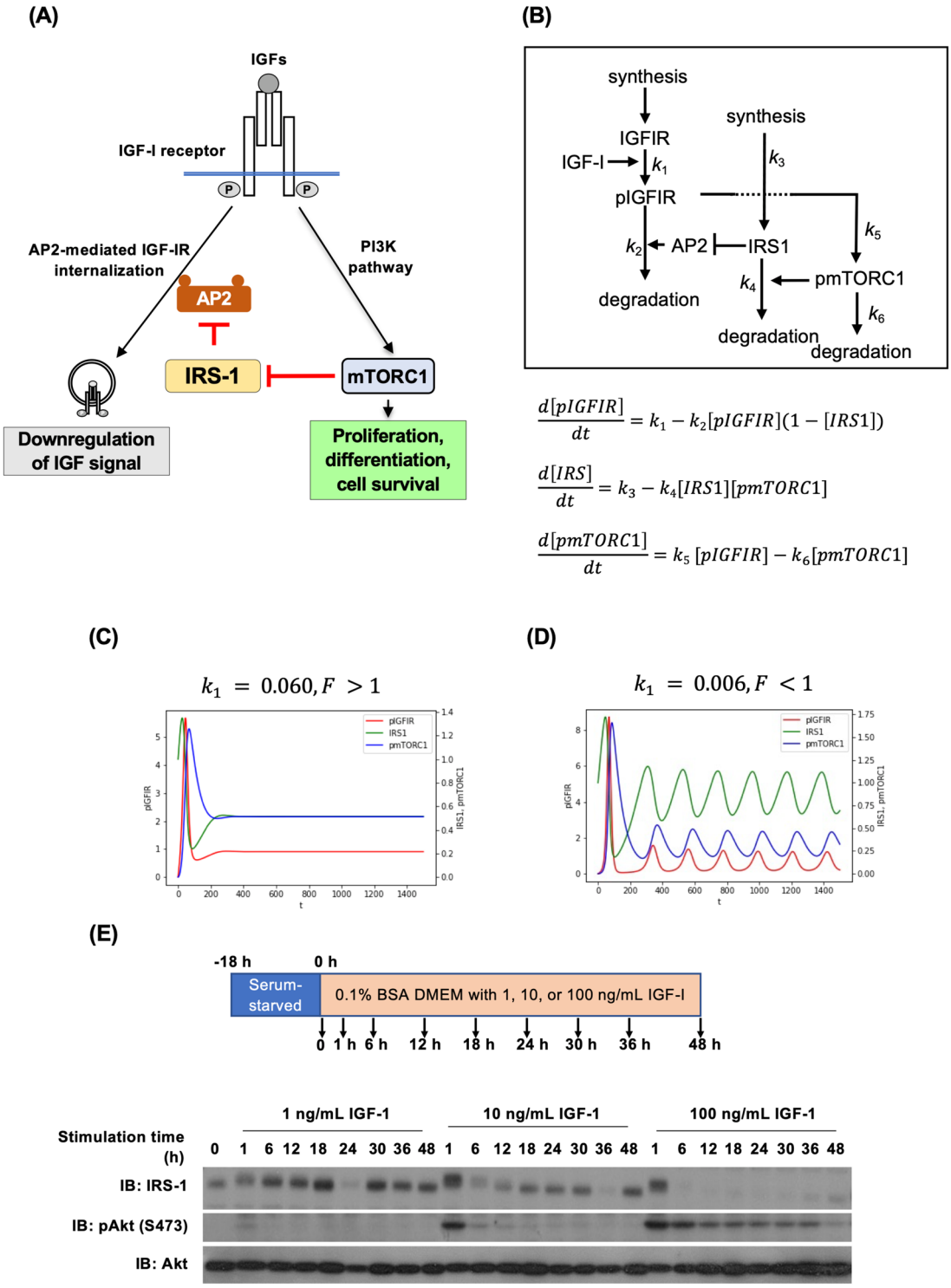

Fig. 2. Mathematical model of the IGF-I signaling pathway. (**A**) Schematic illustration of the IGF-I signaling pathway model. Insulin receptor substrate-1 (IRS-1) inhibits AP2 function, thereby suppressing internalization of the active IGF-I receptor from the plasma membrane. Downstream signaling pathway activation induces the degradation of IRS-1. In this model, IRS-1 is not a mediator but rather a regulator of the IGF signaling pathway. (**B**) A mathematical model based on the IGF-I signaling pathway. (**C,D**) Simulation results of the IGF-I signaling pathway. C: $k_1 = 0.006$. D: $k_1 = 0.06$. (**E**) L6 myoblasts were serum-starved for 18 h, followed by stimulation with DMEM + 2% FBS containing 1 or 100 ng/mL IGF-I. Cell lysates were prepared from each sample, and the total cell lysate was used for immunoblotting analysis with anti-IRS-1, anti-pAkt, or anti-Akt antibodies. *BSA* bovine serum albumin, *mTORC1* mechanistic target of rapamycin complex 1, *PI3K* phosphatidylinositol 3-kinase.

$$\frac{d\boldsymbol{x}}{dt} = \boldsymbol{f}(\boldsymbol{x}, \boldsymbol{k}), \tag{1}$$

where $\boldsymbol{x}$ is a vector of substrates and $\boldsymbol{k}$ is a vector of the parameters. The ordinary differential equations for the three variables in the system are given as follows:

$$\frac{d\left[pIGFIR\right]}{dt} = k_1 - k_2\left[pIGFIR\right](1 - [IRS1]), \tag{2}$$

$$\frac{d[IRS1]}{dt} = k_3 - k_4[IRS1]\left[pmTORC1\right], \tag{3}$$

$$\frac{d\left[pmTORC1\right]}{dt} = k_5\left[pIGFIR\right] - k_6\left[pmTORC1\right]. \tag{4}$$

As shown below, the IGF-I signaling system has a unique equilibrium with nonnegative values:

$$\left(\frac{\alpha\gamma + \beta}{\alpha\beta}, \frac{\alpha\gamma}{\alpha\gamma + \beta}, \frac{\alpha\gamma + \beta}{\alpha\beta\gamma}\right), \tag{5}$$

where

$$\alpha = \frac{k_2}{k_1}, \beta = \frac{k_4}{k_3}, \gamma = \frac{k_6}{k_5}. \tag{6}$$

We performed a linear stability analysis for this equilibrium point. That is, we analytically obtained the Jacobian matrix (J: linearized matrix) at the equilibrium point, and obtained the characteristic polynomial P.

$$J = \begin{bmatrix} -k_2\left(1 - \frac{\alpha\gamma}{\alpha\gamma+\beta}\right) & \frac{k_1(\alpha\gamma+\beta)}{\beta} & 0 \\ 0 & -\frac{k_3(\alpha\gamma+\beta)}{\alpha\gamma} & -\frac{k_4\alpha\gamma}{\alpha\gamma+\beta} \\ k_5 & 0 & -k_6 \end{bmatrix}, \tag{7}$$

$$P = \lambda^3 + \left(\frac{k_2\beta}{\alpha\gamma + \beta} + \frac{k_3(\alpha\gamma + \beta)}{\alpha\gamma} + k_6\right)\lambda^2 + \left(\frac{\alpha\gamma + \beta}{k_2\beta} + \frac{\alpha\gamma}{k_3(\alpha\gamma + \beta)} + \frac{1}{k_6}\right)\alpha\gamma\lambda + \alpha\gamma + \beta. \tag{8}$$

The stability of the equilibrium point is determined by the sign of the real part of the eigenvalues λ of the Jacobian matrix. The eigenvalues are given by the roots of the characteristic equation, $P = 0$. The equation has one negative real root (λ_1) and two complex roots (λ_2 and λ_3). To examine the stability of the point, Hurwitz's stability discriminant method was applied to P. The first and second Hurwitz determinants are always positive, and the third Hurwitz determinant given as:

$$H_3 = \alpha\gamma + \beta - \left(\frac{k_2\beta}{\alpha\gamma + \beta} + \frac{k_3(\alpha\gamma + \beta)}{\alpha\gamma} + k_6\right)\left(\frac{\alpha\gamma + \beta}{k_2\beta} + \frac{\alpha\gamma}{k_3(\alpha\gamma + \beta)} + \frac{1}{k_6}\right)\alpha\gamma. \tag{9}$$

When H_3 is positive, all roots of $P = 0$ have a negative real part, i.e., the equilibrium point is stable. By transforming H_3, we define our criteria of the stability F.

$$F := \frac{\alpha\gamma + \beta}{\left(\frac{k_2\beta}{\alpha\gamma+\beta} + \frac{k_3(\alpha\gamma+\beta)}{\alpha\gamma} + k_6\right)\left(\frac{\alpha\gamma+\beta}{k_2\beta} + \frac{\alpha\gamma}{k_3(\alpha\gamma+\beta)} + \frac{1}{k_6}\right)\alpha\gamma}. \tag{10}$$

Numerical calculations confirmed that at $F = 1$, signs of the real parts of λ_2 and λ_3 switch. The equilibrium point is stable if $F > 1$ but unstable when $F \leqq 1$. Therefore, in this system, Hopf bifurcation occurs at $F = 1$.

As F is a function of k, the stability of the equilibrium switches as k varies (Fig. S1A). Each coefficient of this system was optimized by fitting the experimental results of IRS-1 protein levels and Akt activity (related to pmTORC1 activity) at various time points (0 min, 5 min, 30 min, 60 min, 3 h, 6 h, and 12 h) after stimulation with 100 ng/mL IGF-I (Fig. S2A). For fitting, Bayesian optimization was used. From this optimization process, k_1–k_6 coefficients, could be set, respectively, as shown in Fig. S2B. A comparison of the numerical calculations with optimized coefficient results with the actual values are shown in Fig. S2C. Evaluating the relationship between the k and F values predicted whether IGF-I signaling would oscillate or remain constant (Fig. S3). The values obtained by substituting the optimized coefficients into the F formula are indicated with a white cross symbol in each graph. Furthermore, we showed the change in the F value when coefficients on both axes were altered. In each graph, the F value is shown in the heatmap. A red color indicates that $F > 1$. For example, when k_1 decreases, F decreases. As k_1 is a value that depends on the IGF-I concentration, the IGF-I concentration is a bifurcation parameter that determines whether the IGF-I signaling pathway will oscillate or remain constant. This result can be predicted by referring to the following formula for F: the larger the k_1 value, the larger the F value. Considering that $F < 1$ when $k_1 = 0$, a high IGF-I concentration would stabilize the system with a large F value, whereas a low IGF-I concentration would destabilize the system with a small F value. The simulation results obtained through numerical calculations indicate that IGF-I signaling switches between constant and oscillatory

signals depending on k_1 (Fig. 2C,D). Interestingly, the simulation results indicate that the IGF-I signaling is constant when the optimized k_1 value is used ($k_1 = 0.060$; Fig. 2C). However, when the equivalent k_1 value for the IGF-I concentration is set to one-tenth of the amount ($k_1 = 0.006$), IGF-I signaling oscillates (Fig. 2D). As shown in Fig. 2C, the F value is greater than 1, whereas in Fig. 2D, it is less than 1. Bifurcation diagrams showing the relationship between the k_1 value and amplitude of IRS-1 protein levels are shown in Fig. S1B.

On the other hand, it is accepted by many researchers that IRS-1 is a critical mediator of the IGF-I signaling pathway and that activation of downstream kinase, mTORC1 leads to proteasomal degradation of IRS-1 resulting in suppression of IGF-I signaling activity. We also modeled this canonical IGF-I signaling pathway as differential equation (Fig. S4). This system has two different equilibria, E_+, E_-. Equilibrium point E_- is unstable but exists in a region with negative *[IRS1]*, *[pIRS1]*, and *[pmTORC1]* coordinates. Thus, a state that is impossible in biological phenomena can be realized computationally. On the other hand, equilibrium point E_+ is proved to be always stable under $k > 0$. These data strongly indicated that, in this canonical system, IGF-I signaling activity is always constant.

IGF-I signaling dynamics in L6 myoblasts

To evaluate how the IGF-I signaling pathway was activated in cells, immunoblotting analysis was performed on the L6 myoblasts (Fig. 2E). L6 myoblasts were serum-starved for 18 h, followed by stimulation with 1, 10, or 100 ng/mL IGF-I for the indicated periods. The amount of IRS-1 protein, whose levels were altered in response to IGF-I stimulation, was measured. IRS-1 protein levels increased in all groups after 1 h of IGF-I stimulation. In groups stimulated with 1 ng/mL IGF-I, IRS-1 levels gradually increased for up to 18 h, decreased sharply at 24 h, and then recovered at 30 h. In the groups stimulated with 10 ng/mL IGF-I, IRS-1 levels decreased at 6 h, gradually increased again from 18 to 30 h, decreased at 36 h, and increased thrice at 48 h. Contrarily, in the 100 ng/mL IGF-I-stimulated group, IRS-1 levels decreased at 6 h, and little change was observed. These data indicated that the IGF-I signaling oscillated at a concentration of less than 100 ng/mL IGF-I, whereas the addition of 100 ng/mL IGF-I stabilized it. Contrastingly, activation of Akt, which is related to mTORC1 activity, did not oscillate in all test groups. Because prolonged incubation in serum-free medium is a unideal condition for cells, we performed similar experiments using medium containing 2% FBS. L6 myoblasts were serum-starved for 18 h and stimulated with DMEM 2% FBS containing 0, 1, or 100 ng/mL IGF-I. Stimulation with 2% FBS containing 0 or 1 ng/mL IGF-I made IGF signaling oscillate, but 100 ng/mL IGF-I addition did not (Fig. S5A). Moreover, in mouse C2C12 myoblasts, IRS-1 protein levels and phosphorylated Akt levels were oscillated by stimulation with DEME 2% FBS containing IGF-I (Fig. S5B). In addition, nuclear/cytoplasmic localization of FoxO1 in C2C12 cells under the 100 ng/mL IGF-I stimulation condition was oscillated (Fig. S5C). These experiments data strongly suggested that IGF-I signaling can be oscillated in myoblast under some conditions, and that a model in which IRS-1 is a regulator rather than a mediator (Fig. 2A) is more reliable than a canonical model in which IRS-1 is a mediator (Fig. S4).

Cellular automaton simulation predicted that IRS-1 protein levels oscillate in phase through cell competition during myoblast differentiation

We previously reported that differential expression levels of the IRS-1 protein induce cell competition and that high-level IRS-1 cells are selectively eliminated from cell layers when surrounded by low-level IRS-1 cells[25]. Using cellular automaton analysis, IRS-1 protein levels during the progression of myoblast differentiation were simulated while considering cell competition (Fig. 3A). In this cellular automaton analysis, the cells were shown in a hexagon, and each cell was attached to six other cells. Within each cell, IRS-1 protein levels oscillated in different phases. When the target cell was surrounded by cells with lower levels of IRS-1 (the threshold for the difference in IRS-1 protein levels at which cell competition occurs is set at 0.136; 40% of the amplitude of the oscillation), the target cell was eliminated. The remaining space was then filled by the proliferation of neighboring cells. Detailed conditions under which the cells were eliminated are shown in Fig. 3A. At first, k_1 value was fixed at 0.002, which is around the maximum amplitude of IRS-1 protein level oscillation (Fig. S1B). When the threshold for differences in IRS-1 protein levels at which cell competition occurs was varied, it was observed that lower thresholds resulted in the formation of cell populations with aligned IRS-1 levels (Fig. S6A). In the later analysis, IRS-1 level difference threshold is fixed at 0.136 (40% of amplitude of the oscillation), and the k_1 value was fixed at 0.002. At time 0, each cell had a different IRS-1 protein level because IRS-1 oscillated at different phases ($t = 0$; Fig. 3B). Over time, some cell groups whose IRS-1 protein levels are the same are formed ($t = 20$–140; Fig. 3B). These simulation results indicate that cell competition gradually aligns the IRS-1 levels of neighboring cells, forming cell populations that oscillate during the same phase.

Immunofluorescent analysis revealed synchronized IRS-1 protein oscillations in differentiated myotubes

To confirm this prediction, IRS-1 protein levels in each cell were assessed using immunostaining with an anti-IRS-1 antibody during the progression of myoblast differentiation. Initially, L6 myoblasts were serum-starved for 18 h, stimulated with 100 ng/mL IGF-1, and stained with an anti-IRS-1 antibody (Fig. 3C). Under serum-starved conditions, the fluorescence level of IRS-1 was high, and IRS-1 was mainly localized in nuclei. One hour after IGF-I stimulation, the fluorescence intensity decreased, and the IRS-1 proteins were localized throughout the cell. IRS-1 proteins were exported from nuclei 6 h later and localized mainly in the cytosol. It has been reported that IRS-1 localization was changed in response to IGF-I, but the underlying mechanism remains unknown. Although the relationship between the difference in IRS-1 localization and oscillations of IRS-1 protein level is unclear, these results show that the status of IGF-I signaling activity can be identified by immunostaining of IRS-1. Thus, three types of IRS-1 staining patterns (Type A, B, and C) were identified (Fig. 3C). L6 myoblasts

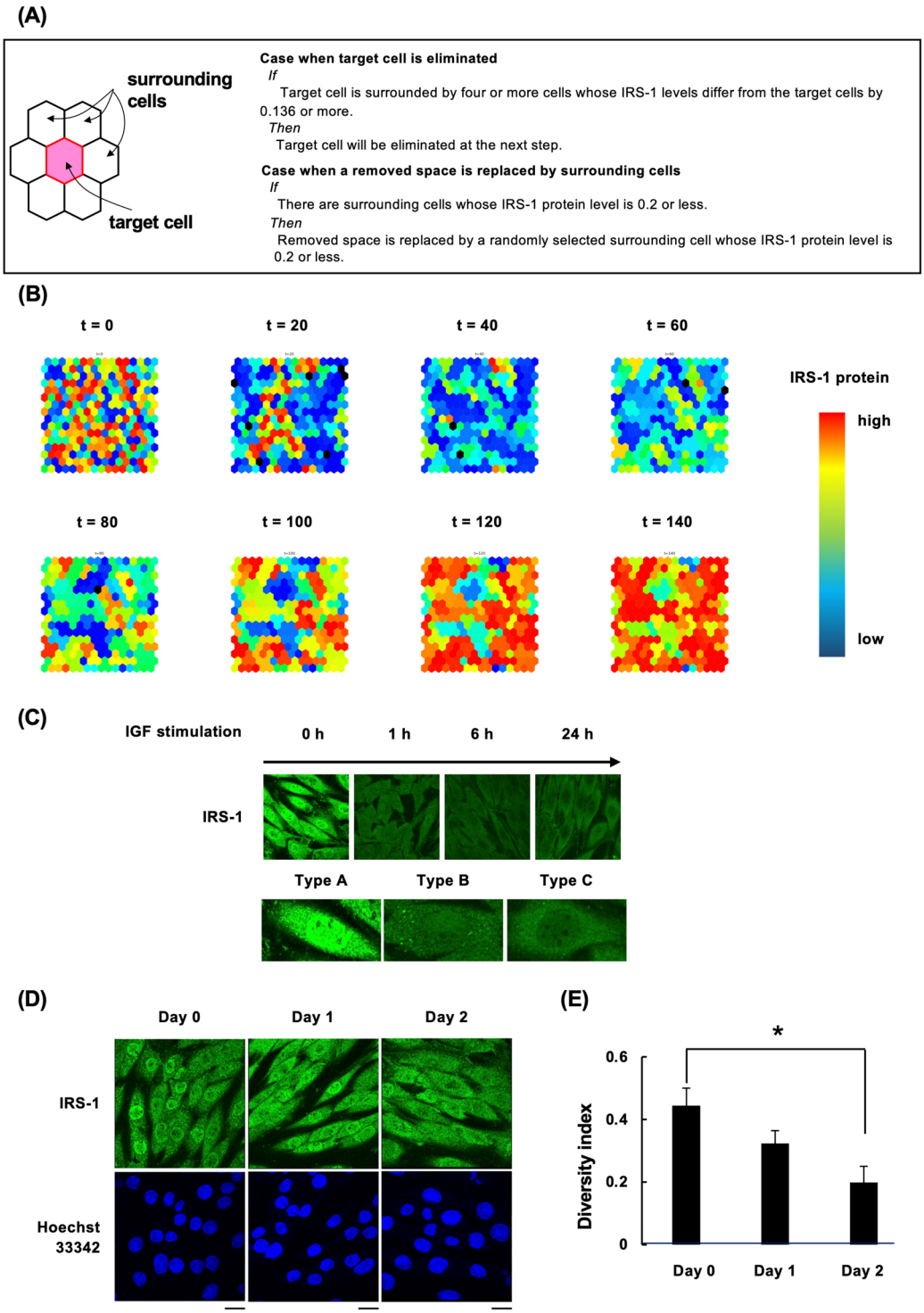

Fig. 3. Synchronization of IGF-I signaling oscillations. (**A**) Cellular automaton-based algorithm considering cell competition. When the target cell is surrounded by low-level IRS-1 cells, target cells are eliminated, and the empty space is replaced by the proliferation of neighboring cells. (**B**) Cellular automaton simulation results. The IRS-1 level in each cell is shown as a heatmap, and the dead space is in black. At time 0, each cell had different IRS-1 protein levels because IRS-1 oscillation was not synchronized. Over time, IRS-1 protein levels gradually synchronized between neighboring cells. (**C**) L6 myoblasts were serum-starved for 18 h, followed by stimulation with 100 ng/mL IGF-I for the indicated time. Afterward, cells were fixed and immunostained with anti-IRS-1 antibody. (**D**) L6 myoblasts were differentiated into myotubes in a differentiation medium. On days 0, 1, or 2 after induction of differentiation, cells were fixed and immunostained with anti-IRS-1 antibody. The green color shows IRS-1, and the blue color indicates the nuclei stained with Hoechst 33342. Scale bar = 20 μm; applicable to all images in each panel. (**E**) The diversity index was calculated from the data of photographs immunostained with IRS-1 and shown as a graph (n = 4). Results are presented as mean ± SEM. *$P < 0.05$. One-way ANOVA and Tukey's post hoc test were performed for assessment.

were differentiated into myotubes by culturing in a differentiation medium. Cells were then immunostained with an anti-IRS-1 antibody at 0, 1, or 2 days after the induction of differentiation (Fig. 3D,E). Before induction of differentiation, the staining pattern of IRS-1 was random. Two days after the induction of differentiation, IRS-1 immunostaining patterns aligned with each other. As mentioned in the "Materials and methods" section, we defined the diversity index as a synchronization parameter and calculated it at 0, 1, and 2 days after the induction of differentiation. Two days after the induction of differentiation, the diversity index decreased significantly, suggesting that the IRS-1 protein oscillation was synchronized after the induction of differentiation.

Synchronization of IGF-I signaling oscillation was critical for myogenic cell fusion to form multinucleate myotubes

To evaluate the biological significance of IGF-I signaling synchronization, cell competition was inhibited by adding an apoptotic inhibitor, Z-VAD-FMK, to the differentiation medium. Addition of Z-VAD-FMK impaired the decrease observed in the diversity index (Fig. 4A), indicating that the synchronization of oscillating IRS-1 levels was inhibited. Z-VAD-FMK addition did not inhibit the expression of MyHC but significantly decreased the fusion index (Fig. 4B). Myomaker plays an important role in myogenic cell fusion[28], and the addition of Z-VAD-FMK was found to decrease its mRNA levels (Fig. 4C). These results indicated that apoptotic inhibitors impeded myogenic cell fusion to form multinucleate myotubes.

Next, we examined whether synchronization of IGF-I signaling oscillations was sufficient for myogenic differentiation. L6 myoblasts were serum-starved for 1 day to synchronize IGF-I signaling oscillation in advance, whereafter differentiation was induced (Fig. 4D). Serum removal before the induction of differentiation clearly accelerated MyHC expression. Interestingly, caspase-3 activation did not enhance after one day under serum-starved conditions. These data strongly suggested that differentiation was accelerated by the pre-synchronization of IGF-I signaling following serum removal.

Synchronization of IGF-I signaling oscillation possibly occurs only under limited IGF concentrations

The relationship between the k_1 value and amplitude of IRS-1 protein oscillation is shown in Figs. S1B and S6B. The k_1 value at which the oscillation and stability switch occurred was approximately 0.0077 (Hopf branch [HB]; Fig. S6B). The amplitude of the IRS-1 protein levels was low when k_1 was close to the HB. Furthermore, as k_1 approached zero, the amplitude of IRS-1 also decreased. Thus, the signaling amplitude was extremely small at IGF-I concentrations near the HB or zero. IGF-I concentrations at which IGF-I signaling oscillated were in the single-digit range, indicating that signaling oscillated only at very limited concentrations. Results of the cellular automaton analysis at various k_1 values are shown in Fig. S6B. When the amplitude of the IRS-1 level is large (when k_1 is between 0.002 and 0.005; very limited concentrations of IGF-I), the amount of IRS-1 in cells becomes synchronized; however, above or below that amount, no synchronization occurs because of the low amplitude of IRS-1 levels.

Discussion

It is well established that IGF-I is an essential hormone for both myoblast proliferation and differentiation. Here, we focused on the difference in IGF-I signaling dynamics at different IGF-I concentrations. Numerical simulation results indicate that IGF-I signaling oscillates at low concentrations and remains stable at high concentrations. Using data from samples treated with 100 ng/mL IGF-I, a k_1 value of 0.067 was calculated to predict approximate IGF-I concentrations. The estimated branching concentration of IGF-I was around 88 ng/mL When k_1 was 0.067 (IGF-I concentration 100 ng/mL), signaling was stable; When k_1 was 0.0067 (IGF-I concentration 10 ng/mL), oscillations occurred, consistent with numerical and experimental findings. Despite its simplicity, the IGF-I signaling model, which used three variables, produced bifurcation analysis results that were consistent with the experiments. Previous data on IRS-1 knockdown not affecting insulin/IGF signaling pathway activation[24,29] and IRS-1 overexpression not enhancing Akt activation could not be reconciled with the previous IRS-1 model as a signaling mediator[30]. However, our current model suggests IRS-1 acts as a signaling modulator, potentially explaining these conflicting observations.

We have some limitations in our IGF-I signaling mathematical model. Some parameters did not align with the fitting data (Fig. S2C). The duration period of the IGF-I signaling oscillation differs between the numerical simulation results and experimental data. Our model is designed to elucidate qualitative dynamics in IGF-I signaling but not for quantitative optimization. Therefore, the accuracy of the fitting data is low, and there are some errors with the duration period of IGF-I signaling oscillation. This error would be the cause of the inconsistency between the timing of the phase alignment of IRS-1 oscillation in the cell and the timing of phase alignment in the cellular automaton analysis. In addition, numerical simulation results predicted that pAkt is also oscillated. However, oscillation could not be observed in the experimental results in L6 myoblasts. We believe that this discrepancy is due to the weak IGF-I signaling activity, which is below the detection limit in Western blotting in L6 so that oscillations cannot be detected; indeed, oscillations in Akt activation and the localization of Foxo1 could be detected in C2C12 cells which has higher IGF-I signaling activation level than L6 (Fig. S5).

The IGF-I signal transduction pathway is similar to that of insulin. However, we can predict that insulin signaling dynamics are different from those of IGFs. As blood insulin levels are transient in the body, insulin bioactivity is transiently expressed and varies continuously in a concentration-dependent manner[31]. Contrarily, blood IGF-I is maintained constantly throughout the day because it has long-running bioactivities, including cell proliferation and cell differentiation[31]. In our study, we showed that the concentration of IGF-I, unlike that of insulin, is a discontinuous switching parameter of signaling dynamics. Data showing that the concentration of IGF-I transformed cell fate and signaling dynamics coincided strongly suggest that IGF signaling dynamics

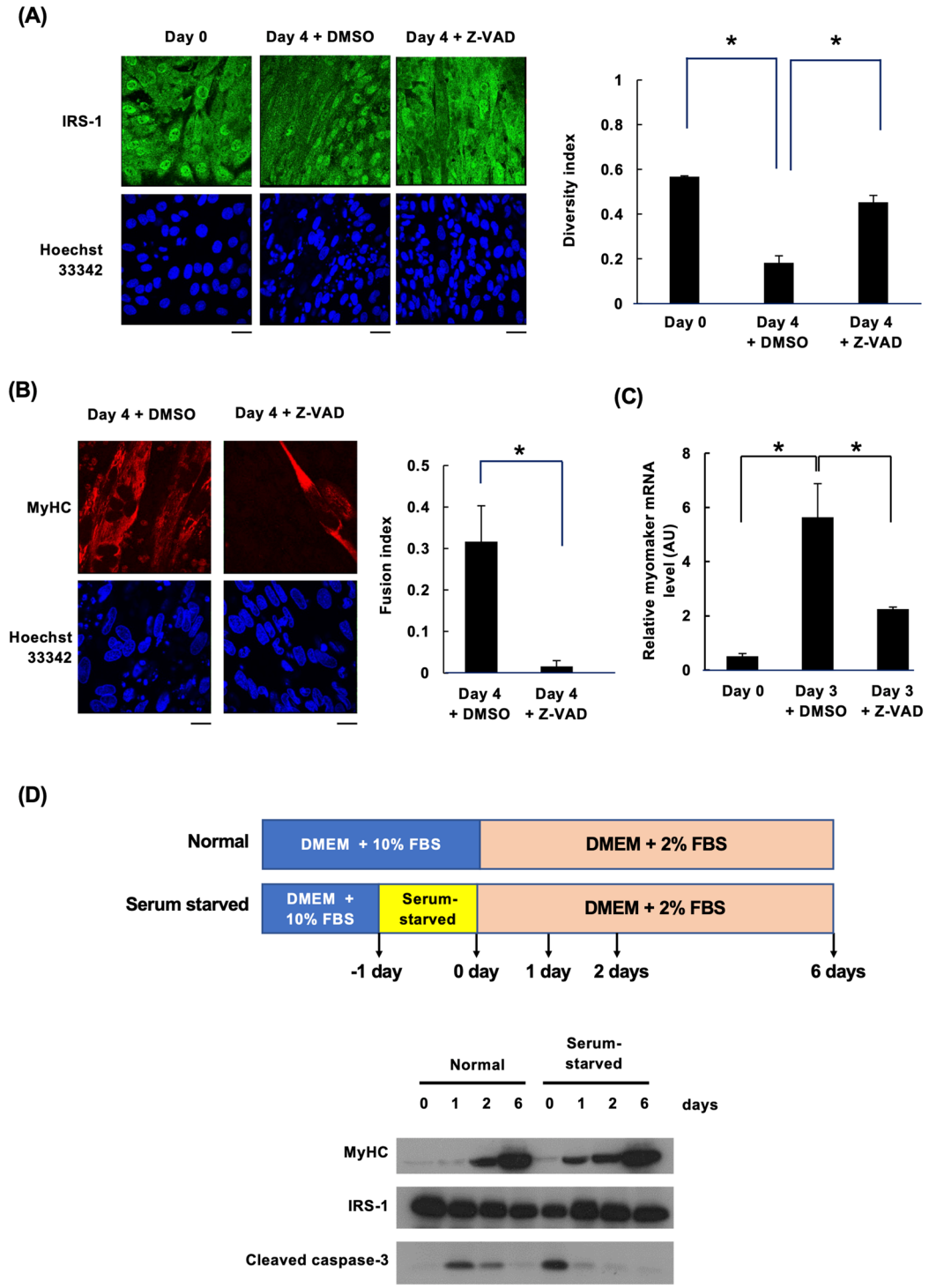

Fig. 4. Synchronization of IRS-1 oscillation is critical for cell fusion. (**A**) L6 myoblast differentiation was induced in the differentiation medium containing Dimethyl sulfoxide (DMSO) or Z-VAD-FMK. At 0 or 4 days after induction of differentiation, cells were fixed and immunostained with an anti-IRS-1 antibody. The green color shows IRS-1, and the blue color indicates the nuclei stained with Hoechst 33342. Scale bar = 50 μm; applicable to all images in each panel. The diversity index was calculated and shown in the graph (n = 4). Results are presented as mean ± SEM. *$P < 0.05$. One-way ANOVA and Tukey's post hoc test were performed for assessment. (**B**) L6 myoblasts were differentiated in the differentiation medium for 4 days. Cells were fixed and immunostained with an anti-MyHC antibody. Scale bar = 20. The fusion index was calculated and shown in the graphs (n = 3). Results are presented as mean ± SEM. *$P < 0.05$. Student's t-test was performed for assessment. (**C**) L6 myoblasts were differentiated in the differentiation medium for 3 days. Myomaker mRNA levels in L6 myoblasts were measured via qPCR (n = 3). Results are presented as mean ± SEM. *$P < 0.05$. One-way ANOVA and Tukey's post hoc test were performed for assessment. (**D**) L6 myoblasts were directly differentiated by exchanging the culture medium from DMEM + 10% FBS to DMEM + 2% FBS (normal). L6 myoblasts were serum-starved for 1 day, followed by differentiation induction in DMEM + 2% FBS. Total cell lysates were prepared for immunoblotting analysis using the indicated antibodies.

determine cell fate. It is well known that myoblasts can differentiate into myotubes or myofibers by changing culture media from DMEM with 20% or 10% FBS to DMEM with 2% FBS or 5% horse serum[14,32]. This is thought to be caused by decreased proliferative activity of some growth factors, such as the epidermal growth factor (EGF) and bFGF[33,34]. However, our report suggested that myoblasts differentiate into myotubes when IGF signaling oscillates after exchanging media from DMEM with 10% FBS to DMEM with 2% FBS; in other words, from a high to a low IGF-I concentration.

IGF-I signaling oscillation is essential for myogenic differentiation as it involves FoxO1 activation. FoxO1, a transcription factor, is excluded from the nucleus and inactivated upon activation of IGF-I signaling[35]. There are reports that active FoxO1 induces myogenic differentiation and that its inactivation is also necessary[35–37]. Additionally, we previously reported that IRS-1 overexpression inhibits myogenic differentiation due to continuous FoxO1 exclusion from nuclei[30]. Sustained FoxO1 inhibition via IGF-I over-addition or IRS-1 overexpression impairs myoblast cell fusion[38–40]. Thus, IGF-I signaling must be suppressed and activated during myogenic differentiation to allow FoxO1 to activate and enhance the transcription of important myogenic proteins. In this study, we have shown that IRS-1 localized in the nucleus was excluded from the nucleus in response to IGF-I stimulation. Although we have reported that differential expression of IRS-1 protein level induced the cell competition, the present results suggest that difference in the subcellular localization of IRS-1 might induce cell competition. Further studies are required in this respect.

Owing to cell competition, cell populations with synchronized IGF-I signaling may fuse to form multinucleated myotubes. Furthermore, an apoptosis inhibitor significantly inhibited the synchronization of IGF-I signaling and myogenic cell fusion. Pre-synchronization of IGF-I signaling by serum starvation enhanced cell differentiation. These results strongly suggest that the synchronization of IGF-I signaling via cell competition is critical for myogenic cell fusion. Myomaker and myomixer are directly involved in cell fusion. Their expression is regulated by typical muscle-specific transcription factors, such as myoblast determination protein 1 (MyoD) and myogenin, as well as by mechanisms that specifically regulate cell fusion, such as ERK5 activation[41,42]. Therefore, the synchronization of IGF-I signaling increasing myomaker expression remains unknown and requires further analysis.

Using the F value, it was possible to uncover a bifurcation parameter to determine IGF-I signaling dynamics (Fig. S4). For example, the IRS-1 production parameter, k_3, is a bifurcation parameter. IGF-I signaling may be constant when k_3 is too high or low. This indicated the possibility that differentiation was inhibited when IRS-1 levels were both too high and low. We have previously reported that IRS-1 overexpression inhibits myogenic differentiation[30]. Such manipulation of IGF-I signaling dynamics could modulate cell fate by artificially changing the coefficients.

There are reports that the localization or activity of some signaling proteins oscillates and that signaling oscillations play essential roles in bioactivity expression. For example, upon EGF stimulation, sustained oscillation of extracellular signal-regulated kinase (ERK) proteins between the nucleus and cytoplasm has been observed[43]. This stochastic ERK activity pulse regulates cell proliferation rates in a density-dependent manner[44,45]. In addition, switch-like ERK activation is essential for invagination of the *Drosophila* tracheal placode[46]. Some reports have shown that Akt phosphorylation in mice fed ad libitum resulted in elevated levels of pAkt at nighttime[47], when the animals normally ingested food. These feeding rhythms were sufficient to generate cycles of Akt phosphorylation. Moreover, these ultradian Akt activation rhythms were observed in a circadian clock-independent manner[47]. Single-cell time-lapse imaging and computational modeling of NF-κB localization showed asynchronous oscillation following signaling stimulation, and the transcription of target genes were dependent on NF-κB oscillation[48]. Thus, the activity and localization of many signaling molecules oscillate; however, regulating signaling dynamics under physiological conditions is unknown. We showed that a slight change in IGF-I concentration controls the oscillations of IGF-I signaling.

This study had some limitations. The IGF-I models created in this study and the validation experiments were mainly performed using L6 myoblasts, and it is unclear whether the dynamics of IGF-I signaling changes in the same manner with IGF-I concentration in different cell lines. Future research must investigate the dynamics of IGF-I signaling in myoblasts via a system that can track IGF-I signaling activity in animal models.

This study concludes that the IGF-I concentration is a bifurcation parameter that determines cell fate by switching IGF-I signaling dynamics. High IGF-I levels inhibited myogenesis owing to constant IGF-I signaling. When the IGF-I level was low, synchronization of IGF-I signaling failed because of the low amplitude of IRS-1 protein levels (Fig. S5). These results indicated that myogenic differentiation was induced only at a limited IGF-I concentration. This system may be an excellent cell-autonomous system in which IGF-I controls the oscillation of IGF-I signaling and the amplitude of IRS-1 level oscillations, ensuring that cells do not easily induce muscle differentiation.

Materials and methods

Materials

DMEM and phosphate-buffered saline (PBS) were purchased from Nissui Pharmaceutical Co. (Tokyo, Japan). FBS was obtained from Sigma-Aldrich (St. Louis, MO, USA), and IGF-I from Wako Chemicals (Tokyo, Japan). Penicillin and streptomycin were obtained from Banyu Pharmaceutical Co. (Tokyo, Japan). Polyclonal anti-IRS-1 antibodies for immunoblotting and immunostaining were obtained from Merck Millipore (Middlesex Country, MA, USA) and ProteinTech (Tokyo, Japan), respectively. Anti-caspase-3 antibody was purchased from Cell Signaling Technology (Danvers, MA, USA), and anti-MyHC antibody from Merck Millipore. Hoechst 33342 was purchased from Molecular Probes (Eugene, OR, USA) and z-VAD-FMK from BD Biosciences (Franklin Lakes, NJ, USA). Horseradish peroxidase-conjugated secondary anti-rabbit and anti-mouse IgG antibodies were obtained from GE Healthcare (Pittsburgh, PA, USA). Enhanced chemiluminescence reagents were obtained

from PerkinElmer Life Sciences (Boston, MA, USA). All other chemicals used were of reagent grade and commercially available.

Cell cultures and differentiation

L6 myoblasts were purchased from the American Type Tissue Culture Collection (Manassas, VA, USA). L6 myoblasts were maintained at 37 °C in a humidified, 5% CO_2-controlled atmosphere in DMEM supplemented with 10% FBS, 0.1% $NaHCO_3$, 50 IU/mL penicillin, and 50 µg/mL streptomycin. L6 differentiation was induced as described previously[30].

Immunoblotting analysis

Cells were lysed at 4 °C with ice-cold lysis buffer (1% NP40, 50 mM Tris–HCl [pH 7.4], 150 mM NaCl, 1 mM EDTA, 1 mM NaF, 10% glycerol, 20 µg/mL phenylmethylsulfonyl fluoride [PMSF], 5 µg/mL pepstatin, 10 µg/mL leupeptin, 100 KIU/mL aprotinin, 1 mM Na_3VO_4, and 10 mg/mL *p*-nitrophenyl phosphate) or ice-cold Ristocetin-induced platelet aggregation (RIPA) buffer (50 mM Tris–HCl [pH 7.4], 15 mM NaCl, 0.1% sodium dodecyl sulfate [SDS], 0.5% deoxycholate, 20 µg/mL PMSF, 5 µg/mL pepstatin, 10 µg/mL leupeptin, 100 KIU/mL aprotinin, 1 mM Na_3VO_4, and 10 mg/mL *p*-nitrophenyl phosphate). Insoluble materials were removed via centrifugation at 15,000×*g* for 10 min at 4 °C, and the supernatant was prepared as the total cell lysate. Immunoblotting was performed as described previously[13].

Mathematical model of the IGF signaling pathway

We constructed a mathematical model of the IGF-I signaling pathway, as shown in Fig. 2A,B. Here, we describe the activation of the IGF-I receptor with IGF-I treatment, denoted by *[pIGFIR]*. The rate at which insulin-like growth factor-I receptor (IGFIR) is activated is:

$$\frac{K[IGFIR][IGF1]}{(1+K[IGFIR])} = k_1,$$

where *[IGFIR]* represents the amount of IGF-I receptors on the plasma membrane, *[IGF1]* is the concentration of IGF-I in the medium, and K is the coupling constant for IGFIR and IGF-I. We have previously reported that IGF-I receptor levels on the plasma membrane were not altered after IGF-I stimulation[24]. Therefore, for simplicity, we used the rate at which IGFIR is activated as the constant, k_1. This implies that k_1 corresponds to the IGF-1 concentration.

Parameter fitting of IGF signaling pathway

Each coefficient of the IGF signaling pathway system was optimized by fitting the experimental results of IRS-1 protein levels and Akt activity (related to pmTORC1 activity). Bayesian optimization was employed to fit the coefficients based on experimentally obtained values. This method utilizes previous experimental outcomes to determine experimental parameters from probability distributions, aiming to identify optimal hyperparameters with minimal trial iterations.

Thymidine incorporation into DNA

L6 cells in 48-well plates were cultured for 24 h in differentiation medium containing the indicated concentrations of IGF-I. [Methyl-^{3}H] thymidine (0.3 µCi/well, 1 µCi/mL; GE Healthcare) was added to each well 4 h before the termination of each experiment. Labeling was terminated by adding 500 µL of 1 M ascorbic acid. The cells were washed twice with ice-cold PBS and twice with ice-cold 10% trichloroacetic acid. Trichloroacetic acid-precipitated materials were solubilized with 250 µL of 0.2 N NaOH and 0.1% SDS, mixed into 5 mL clear-sol II (Nacalai Tesque, Kyoto, Japan), and radioactivity measured with a liquid scintillation counter (Perkin Elmer).

Immunofluorescence staining

For confocal microscopy analysis, L6 cells were grown on coverslips. The cells were fixed for 10 min at 25 °C in prewarmed 4% paraformaldehyde in PBS. After washing three times with PBS, cells were permeabilized with 0.25% Triton X-100 in PBS at 25 °C for 10 min. The cells were washed three times with PBS and then blocked for 1 h at 4 °C with bovine serum albumin (BSA) blocking buffer (3% BSA and 0.025% NaN_3 in PBS). Primary antibodies diluted in BSA blocking buffer were added overnight at 4 °C. The samples were washed three times with PBS and incubated for 1 h at 25 °C in a solution of Alexa Fluor-conjugated secondary antibodies diluted in BSA blocking buffer. The coverslips were mounted using Vectashield for visualization under fluorescence (Keyence, Tokyo, Japan) and confocal fluorescence microscopes (Olympus, Tokyo, Japan).

Cellular automaton analysis

Synchronization of IGF-I signaling during myogenic differentiation was simulated using the cellular automaton program. The algorithm used to simulate cell competition is shown in Fig. 3A.

Fusion index

The fusion index was determined by dividing the number of nuclei in myotubes composed of at least three cells by the total number of nuclei observed in each fluorescence micrograph.

Diversity index

L6 myoblasts were induced to differentiate into myotubes. On the indicated days after the induction of differentiation, the cells were immunostained with an anti-IRS-1 antibody. The staining pattern of each cell was classified as A–C, and the number of boundaries (Nb) of all cells in the fluorescence micrographs was counted. If the staining patterns of two neighboring cells differed, 1 was added; if they were the same, 0 was added. This was performed at the boundaries of all cells. The resulting value (Db) was then used to calculate the diversity index with the following formula:

$$Diversity\ index = \frac{Db}{2 \times Nb}.$$

Statistical analysis

All data are defined within the figure legends. Comparisons between two groups were performed using Student's t-test, whereas comparisons between more than two groups were analyzed via one-way analysis of variance (ANOVA) and Tukey's post hoc test.

Data availability

All relevant data are available from the lead contact, Fumihiko Hakuno (hakuno@g.ecc.u-tokyo.ac.jp), upon request.

Received: 1 February 2024; Accepted: 30 August 2024
Published online: 05 September 2024

References

1. Nakae, J., Kido, Y. & Accili, D. Distinct and overlapping functions of insulin and IGF-I receptors. *Endocr. Rev.* **22**, 818–835. https://doi.org/10.1210/EDRV.22.6.0452 (2001).
2. Fukushima, T. *et al.* Phosphatidylinositol 3-kinase (PI3K) activity bound to insulin-like growth factor-I (IGF-I) receptor, which is continuously sustained by IGF-I stimulation, is required for IGF-I-induced cell proliferation. *J. Biol. Chem.* **287**, 29713–29721. https://doi.org/10.1074/jbc.M112.393074 (2012).
3. Dumont, N. A., Bentzinger, C. F., Sincennes, M. C. & Rudnicki, M. A. Satellite cells and skeletal muscle regeneration. *Compr. Physiol.* **5**, 1027–1059. https://doi.org/10.1002/CPHY.C140068 (2015).
4. Clemmons, D. R. Role of IGF-I in skeletal muscle mass maintenance. *Trends Endocrinol. Metab.* **20**, 349–356. https://doi.org/10.1016/J.TEM.2009.04.002 (2009).
5. Barton-Davis, E. R., Shoturma, D. I. & Sweeney, H. L. Contribution of satellite cells to IGF-I induced hypertrophy of skeletal muscle. *Acta Physiol. Scand.* **167**, 301–305. https://doi.org/10.1046/J.1365-201X.1999.00618.X (1999).
6. Edwall, D., Schalling, M., Jennische, E. & Norstedt, G. Induction of insulin-like growth factor I messenger ribonucleic acid during regeneration of rat skeletal muscle. *Endocrinology* **124**, 820–825. https://doi.org/10.1210/ENDO-124-2-820 (1989).
7. Coleman, M. E. *et al.* Myogenic vector expression of insulin-like growth factor I stimulates muscle cell differentiation and myofiber hypertrophy in transgenic mice. *J. Biol. Chem.* **270**, 12109–12116. https://doi.org/10.1074/JBC.270.20.12109 (1995).
8. Liu, J. P., Baker, J., Perkins, A. S., Robertson, E. J. & Efstratiadis, A. Mice carrying null mutations of the genes encoding insulin-like growth factor I (Igf-1) and type 1 IGF receptor (Igf1r). *Cell* **75**, 59–72. https://doi.org/10.1016/S0092-8674(05)80084-4 (1993).
9. Florini, J. R., Ewton, D. Z., Magri, K. A. & Mangiacapra, F. J. IGFs and muscle differentiation. *Adv. Exp. Med. Biol.* **343**, 319–326. https://doi.org/10.1007/978-1-4615-2988-0_31 (1993).
10. Duan, C., Ren, H. & Gao, S. Insulin-like growth factors (IGFs), IGF receptors, and IGF-binding proteins: Roles in skeletal muscle growth and differentiation. *Gen. Comp. Endocrinol.* **167**, 344–351. https://doi.org/10.1016/J.YGCEN.2010.04.009 (2010).
11. Tollefsen, S. E., Lajara, R., McCusker, R. H., Clemmons, D. R. & Rotwein, P. Insulin-like growth factors (IGF) in muscle development. Expression of IGF-I, the IGF-I receptor, and an IGF binding protein during myoblast differentiation. *J. Biol. Chem.* **264**, 13810–13817. https://doi.org/10.1016/S0021-9258(18)80073-4 (1989).
12. Tureckova, J., Wilson, E. M., Cappalonga, J. L. & Rotwein, P. Insulin-like growth factor-mediated muscle differentiation: Collaboration between phosphatidylinositol 3-kinase-Akt-signaling pathways and myogenin. *J. Biol. Chem.* **276**, 39264–39270. https://doi.org/10.1074/jbc.M104991200 (2001).
13. Yoneyama, Y. *et al.* The AP-1 complex regulates intracellular localization of insulin receptor substrate 1, which is required for insulin-like growth factor I-dependent cell proliferation. *Mol. Cell. Biol.* **33**, 1991–2003. https://doi.org/10.1128/MCB.01394-12 (2013).
14. Florini, J. R., Ewton, D. Z. & Coolican, S. A. Growth hormone and the insulin-like growth factor system in myogenesis. *Endocr. Rev.* **17**, 481–517. https://doi.org/10.1210/edrv-17-5-481 (1996).
15. Florini, J. R., Ewton, D. Z., Falen, S. L. & Van Wyk, J. J. Biphasic concentration dependency of stimulation of myoblast differentiation by somatomedins. *Am. J. Physiol.* **250**, C771–C778. https://doi.org/10.1152/ajpcell.1986.250.5.C771 (1986).
16. Grønborg, M., Wulff, B. S., Rasmussen, J. S., Kjeldsen, T. & Gammeltoft, S. Structure-function relationship of the insulin-like growth factor-I receptor tyrosine kinase. *J. Biol. Chem.* **268**, 23435–23440. https://doi.org/10.1016/S0021-9258(19)49481-7 (1993).
17. Ullrich, A. & Schlessinger, J. Signal transduction by receptors with tyrosine kinase activity. *Cell* **61**, 203–212. https://doi.org/10.1016/0092-8674(90)90801-k (1990).
18. Yenush, L. & White, M. F. The IRS-signalling system during insulin and cytokine action. *BioEssays* **19**, 491–500. https://doi.org/10.1002/bies.950190608 (1997).
19. Backer, J. M. *et al.* Phosphatidylinositol 3′-kinase is activated by association with IRS-1 during insulin stimulation. *EMBO J.* **11**, 3469–3479. https://doi.org/10.1002/j.1460-2075.1992.tb05426.x (1992).
20. Myers, M. G. *et al.* IRS-1 activates phosphatidylinositol 3′-kinase by associating with Src homology 2 domains of p85. *Proc. Natl Acad. Sci. U.S.A.* **89**, 10350–10354. https://doi.org/10.1073/pnas.89.21.10350 (1992).
21. Dummler, B. & Hemmings, B. A. Physiological roles of PKB/Akt isoforms in development and disease. *Biochem. Soc. Trans.* **35**, 231–235. https://doi.org/10.1042/BST0350231 (2007).
22. Lee, A. V., Gooch, J. L., Oesterreich, S., Guler, R. L. & Yee, D. Insulin-like growth factor I-induced degradation of insulin receptor substrate 1 is mediated by the 26S proteasome and blocked by phosphatidylinositol 3′-kinase inhibition. *Mol. Cell. Biol.* **20**, 1489–1496. https://doi.org/10.1128/MCB.20.5.1489-1496.2000 (2000).
23. Yoneyama, Y. *et al.* Serine phosphorylation by mTORC1 promotes IRS-1 degradation through SCFβ-TRCP E3 ubiquitin ligase. *iScience* **5**, 1–18. https://doi.org/10.1016/j.isci.2018.06.006 (2018).

24. Yoneyama, Y. *et al.* IRS-1 acts as an endocytic regulator of IGF-I receptor to facilitate sustained IGF signaling. *ELife* **7**, 893. https://doi.org/10.7554/eLife.32893 (2018).
25. Okino, R., Usui, A., Yoneyama, Y., Takahashi, S. I. & Hakuno, F. Myoblasts with higher IRS-1 levels are eliminated from the normal cell layer during differentiation. *Front. Endocrinol.* **11**, 96. https://doi.org/10.3389/fendo.2020.00096 (2020).
26. Simpson, P. & Morata, G. Differential mitotic rates and patterns of growth in compartments in the Drosophila wing. *Dev. Biol.* **85**, 299–308. https://doi.org/10.1016/0012-1606(81)90261-x (1981).
27. Morata, G. Cell competition: A historical perspective. *Dev. Biol.* **476**, 33–40. https://doi.org/10.1016/J.YDBIO.2021.02.012 (2021).
28. Leikina, E. *et al.* Myomaker and Myomerger work independently to control distinct steps of membrane remodeling during myoblast fusion. *Dev. Cell* **46**, 767–780. https://doi.org/10.1016/J.DEVCEL.2018.08.006 (2018).
29. Sasaki-Suzuki, N. *et al.* Growth hormone inhibition of glucose uptake in adipocytes occurs without affecting GLUT4 translocation through an insulin receptor substrate-2-phosphatidylinositol 3-kinase-dependent pathway. *J. Biol. Chem.* **284**, 6061–6070. https://doi.org/10.1074/jbc.M808282200 (2009).
30. Hakuno, F. *et al.* Constitutive expression of insulin receptor substrate (IRS)-1 inhibits myogenic differentiation through nuclear exclusion of FoxO1 in L6 myoblasts. *PLoS ONE* **6**, e25655. https://doi.org/10.1371/journal.pone.0025655 (2011).
31. Hakuno, F. & Takahashi, S. I. IGF1 receptor signaling pathways. *J. Mol. Endocrinol.* **61**, T69–T86. https://doi.org/10.1530/JME-17-0311 (2018).
32. Florini, J. R. *et al.* 'Spontaneous' differentiation of skeletal myoblasts is dependent upon autocrine secretion of insulin-like growth factor-II. *J. Biol. Chem.* **266**, 15917–15923. https://doi.org/10.1016/S0021-9258(18)98496-6 (1991).
33. Leroy, M. C., Perroud, J., Darbellay, B., Bernheim, L. & Konig, S. Epidermal growth factor receptor down-regulation triggers human myoblast differentiation. *PLoS ONE* **8**, e71770. https://doi.org/10.1371/JOURNAL.PONE.0071770 (2013).
34. Riuzzi, F., Sorci, G. & Donato, R. S100B protein regulates myoblast proliferation and differentiation by activating FGFR1 in a bFGF-dependent manner. *J. Cell Sci.* **124**, 2389–2400. https://doi.org/10.1242/JCS.084491 (2011).
35. Hribal, M. L., Nakae, J., Kitamura, T., Shutter, J. R. & Accili, D. Regulation of insulin-like growth factor-dependent myoblast differentiation by foxo forkhead transcription factors. *J. Cell Biol.* **162**, 535–541. https://doi.org/10.1083/jcb.200212107 (2003).
36. Wu, A. L., Kim, J. H., Zhang, C., Unterman, T. G. & Chen, J. Forkhead box protein O1 negatively regulates skeletal myocyte differentiation through degradation of mammalian target of rapamycin pathway components. *Endocrinology* **149**, 1407–1414. https://doi.org/10.1210/EN.2007-1470 (2008).
37. Kitamura, T. *et al.* A Foxo/Notch pathway controls myogenic differentiation and fiber type specification. *J. Clin. Investig.* **117**, 2477–2485. https://doi.org/10.1172/JCI32054 (2007).
38. Bois, P. R. J. & Grosveld, G. C. FKHR (FOXO1a) is required for myotube fusion of primary mouse myoblasts. *EMBO J.* **22**, 1147–1157. https://doi.org/10.1093/EMBOJ/CDG116 (2003).
39. Nishiyama, T., Kii, I. & Kudo, A. Inactivation of rho/ROCK signaling is crucial for the nuclear accumulation of FKHR and myoblast fusion. *J. Biol. Chem.* **279**, 47311–47319. https://doi.org/10.1074/jbc.M403546200 (2004).
40. Xu, M., Chen, X., Chen, D., Yu, B. & Huang, Z. FoxO1: A novel insight into its molecular mechanisms in the regulation of skeletal muscle differentiation and fiber type specification. *Oncotarget* **8**, 10662–10674. https://doi.org/10.18632/ONCOTARGET.12891 (2017).
41. Luo, W., Li, E., Nie, Q. & Zhang, X. Myomaker, regulated by MYOD, MYOG and miR-140-3p, promotes chicken myoblast fusion. *Int. J. Mol. Sci.* **16**, 26186–26201. https://doi.org/10.3390/ijms161125946 (2015).
42. Sunadome, K. *et al.* ERK5 regulates muscle cell fusion through Klf transcription factors. *Dev. Cell* **20**, 192–205. https://doi.org/10.1016/J.DEVCEL.2010.12.005 (2011).
43. Shankaran, H. *et al.* Rapid and sustained nuclear–cytoplasmic ERK oscillations induced by epidermal growth factor. *Mol. Syst. Biol.* **5**, 332–332. https://doi.org/10.1038/MSB.2009.90 (2009).
44. Yang, J. M. *et al.* Integrating chemical and mechanical signals through dynamic coupling between cellular protrusions and pulsed ERK activation. *Nat. Commun.* **9**, 4673. https://doi.org/10.1038/s41467-018-07150-9 (2018).
45. Aoki, K. *et al.* Stochastic ERK activation induced by noise and cell-to-cell propagation regulates cell density-dependent proliferation. *Mol. Cell* **52**, 529–540. https://doi.org/10.1016/J.MOLCEL.2013.09.015 (2013).
46. Ogura, Y., Wen, F. L., Sami, M. M., Shibata, T. & Hayashi, S. A switch-like activation relay of EGFR-ERK signaling regulates a wave of cellular contractility for epithelial invagination. *Dev. Cell* **46**, 162–172. https://doi.org/10.1016/J.DEVCEL.2018.06.004 (2018).
47. Vollmers, C. *et al.* Time of feeding and the intrinsic circadian clock drive rhythms in hepatic gene expression. *Proc. Natl. Acad. Sci. U.S.A.* **106**, 21453–21458. https://doi.org/10.1073/PNAS.0909591106 (2009).
48. Nelson, D. E. *et al.* Oscillations in NF-kappaB signaling control the dynamics of gene expression. *Science* **306**, 704–708. https://doi.org/10.1126/science.1099962 (2004).

Acknowledgements

The authors would like to thank Editage (www.Editage.jp) for English language editing. This work was supported in part by the Grants-in-Aid for Scientific Research [Scientific Research (B) #24380152, (B) #15H04583, and (B) #22H02528 to F.H. and Scientific Research (A) #16208028, (A) #22248030, and (S) #25221204 to S.-I.T.]; the Cross-ministerial Moonshot Agriculture, Forestry, and Fisheries Research and Development Program, "Technologies for Smart Bio-industry and Agriculture," from the Bio-oriented Technology Research Advancement Institution, NARO (Grant Number: 20350956); and the Core-to-Core program from the Japan Society for the Promotion of Science (Grant Number: JPJSCCA20210007 to S.-I.T).

Author contributions

Conceptualization, R.O. and F.H.; Methodology, R.O., K.M., S.O., and F.H.; Software, M.M., K.M., S.W., A.M., and F.H.; Validation, R.O., K.M., S.W., A.M., S.O., and F.H.; Investigation, R.O., K.M., S.W., A.M., and F.H.; Resources, S.N. and Y.Y.; Writing—Original Draft, R.O., K.M., and F.H.; Writing—Review & Editing, R.O., K.M., A.M., T.M., Y.Y., S.T. and F.H.; Funding Acquisition, S.T. and F.H.

Competing interests

The authors declare no competing interests.

Additional information

Supplementary Information The online version contains supplementary material available at https://doi.org/10.1038/s41598-024-71739-y.

Correspondence and requests for materials should be addressed to F.H.